Materials Transactions, Vol. 54, No. 8 (2013) pp. 1314 to 1323
Special Issue on Advanced Materials Development and Integration of Novel Structured Metallic and Inorganic Materials

Recent Progress in Ti-Based Metallic Glasses for Application as Biomaterials

Guoqiang Xie*, Fengxiang Qin and Shengli Zhu

Institute for Materials Research, Tohoku University, Sendai 980-8577, Japan

Ti-based bulk metallic glasses are of great interest in biomedical applications due to their high corrosion resistance, excellent mechanical properties and good biocompatibility. This article reviews recent progress in the development of Ti-based metallic glasses for the application as biomaterials. Ti-based (Ti–Zr–Cu–Pd, Ti–Zr–Cu–Pd–Sn, and Ti–Zr–Cu–Pd–Nb) bulk metallic glasses without toxic and allergic elements have been developed. These glassy alloys exhibited high glass-forming ability, high strength, large plasticity, good corrosion resistance and excellent biocompatibility, which open possibilities to create Ti-based metallic glass implants. Using a spark plasma sintering process, large-size Ti-based bulk metallic glasses and the composites with hydroxyapatite, as well as porous glassy alloys having approximate Young's modulus with that of bone were developed. [doi:10.2320/matertrans.MF201315]

(Received February 7, 2013; Accepted April 5, 2013; Published May 24, 2013)

Keywords: *titanium-based metallic glass, biomaterials, bioactivity, mechanical properties, corrosion resistance*

1. Introduction

Metallic materials owing to their excellent mechanical strength and resilience show a great potential for replacing failed hard tissue, and are superior in many aspects to alternative biomaterials such as ceramics and polymers. To assure long life-time of the load-bearing orthopedic implants, biomaterials need to satisfy the following requirements:[1–3] (1) They should not contain toxic or non-biocompatible elements (*e.g.*, Ni or Be), and this places stringent restriction to the choice of alloying elements. (2) Their long service life coupled with the variety of human activity demands excellent mechanical properties, primarily high strength and high fatigue resistance, but low elastic modulus. This is a big challenge because for crystalline materials their strength and elastic modulus tend to increase or decrease simultaneously. (3) Wear resistance is important because wear causes not only implant loosening but also harmful reactions if the wear debris is deposited in the tissue. (4) Biochemical compatibility requires the implanted materials to possess superior corrosion resistance in body environment and be bioactive. Presently, the materials used for these applications are 316 L stainless steel, cobalt chromium alloys, and titanium-based alloys. Unfortunately, these materials have exhibited tendencies to fail after long-term use due to various reasons.[3,4]

Bulk metallic glasses (BMGs) have been rapidly developed in the past two decades in many alloy systems because of their unique excellent physical, chemical, and mechanical properties compared with conventional crystalline alloys such as high strength, high elastic limit, low Young's modulus and excellent corrosion and wear resistances.[5–7] Among the glassy alloys, Ti-based BMGs are expected to be applied as biomedical materials. Many Ti-based BMGs have been developed in the framework of the Ti–Ni–Cu,[8–17] Ti–Zr–Be[18–21] and Ti–Zr–Cu–Ni[22–25] alloy systems, based on the Inoue's three empirical rules,[26–28] i.e., (1) multi-component consisting of more than three elements, (2) significant atomic size mismatches above 12% among the main three elements, and (3) negative heats of mixing among the main elements. However, these Ti-based BMGs contain Ni and/or Be, etc., which are not suitable to be in contact with human body because of the cytotoxicity, limiting the application of Ti-based BMGs in biomedical fields. The solute elements like Ni, Be, etc., leading to the decrease in the critical cooling rate are known as essential alloying elements for fabrication of Ti-based BMGs. So it is of scientific and technological interest to synthesize new Ti-based BMGs free to toxic elements. This paper reviews recent results on development of the Ni- and Be-free Ti-based BMGs for biomedical applications.

2. Development of Ti-Based Metallic Glasses with Potential for Biomaterial Applications

2.1 Ni- and Be-free Ti-based bulk metallic glasses

Since Pd and Ni belong to the same family in an element periodic table, the replacement of Ni by Pd has been explored. The Ti–Zr–Cu–Pd quaternary bulk glassy alloys without toxic and allergic elements such as Ni and Be have been developed.[29,30] Figure 1 shows the composition de-

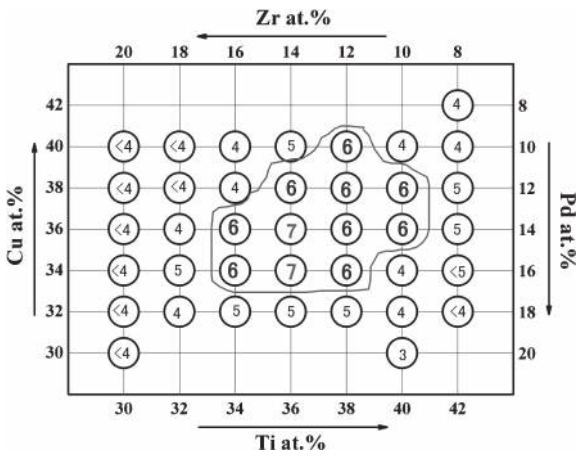

Fig. 1 Critical diameters (mm) of Ti–Zr–Cu–Pd glassy alloy rods produced by copper mold casting.[29]

*Corresponding author, E-mail: xiegq@imr.tohoku.ac.jp

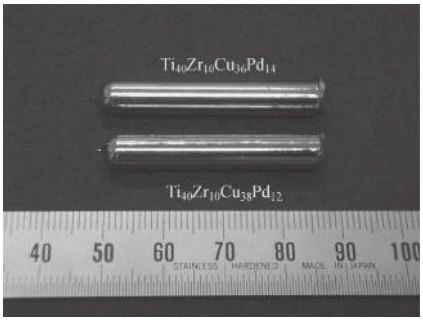

Fig. 2 Outer surface of cast $Ti_{40}Zr_{10}Cu_{36}Pd_{14}$ and $Ti_{40}Zr_{10}Cu_{38}Pd_{12}$ bulk glassy alloy rods with a diameter of 6 mm.[30]

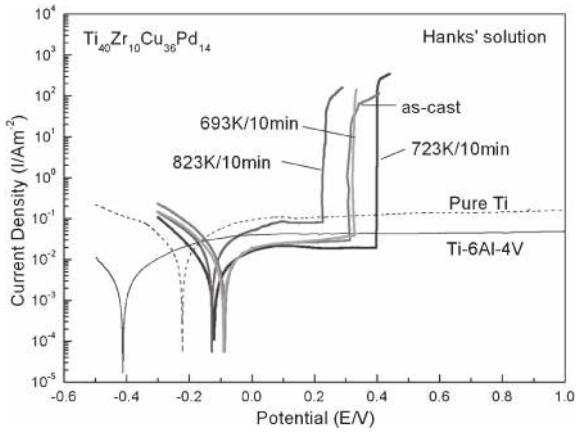

Fig. 3 Anodic and cathodic polarization curves of the $Ti_{40}Zr_{10}Cu_{36}Pd_{14}$ bulk glassy alloy of the as-cast and via annealing treatment immersed in Hanks' solution at 310 K. The curves of pure Ti and Ti–6Al–4V alloy are also shown for comparison.[31]

pendence of critical diameters (d_c) of Ti–Zr–Cu–Pd glassy alloy rods produced by copper mold casting.[29] The Ti–Zr–Cu–Pd glassy alloys exhibit high glass-forming ability (GFA) (with critical diameters of 7 mm) and relatively large supercooled liquid region (ΔT_X) of over 50 K. The $Ti_{40}Zr_{10}Cu_{36}Pd_{14}$ glassy alloy had the highest GFA. The compressive strength and the Young's modulus were 1950 MPa and 82 GPa, respectively.[30] Figure 2 shows typical outer appearance of the Ti–Zr–Cu–Pd glassy alloy rods. The results of potentiodynamic polarization measurements revealed that the $Ti_{40}Zr_{10}Cu_{36}Pd_{14}$ glassy alloy was spontaneously passivated by anodic polarization in Hanks' solution, as shown in Fig. 3.[31] The passive current density of as-cast $Ti_{40}Zr_{10}Cu_{36}Pd_{14}$ glassy alloy is about 10^{-2} Am^{-2}. It is lower than that of pure Ti and commercial Ti–6Al–4V alloy, indicating that more protective and denser passive film is formed on the surface of the Ti-based glassy alloy in the anodic process before onset potential of the pitting.

2.2 Improvement of mechanical and corrosion properties

Bulk metallic glasses usually exhibit low plasticity due to the absence of dislocation activity and the rapid propagation of few shear bands throughout the sample under application of mechanical stress. Like most metallic glasses, the Ti–Zr–Cu–Pd glassy alloys also exhibit low plasticity. Several strategies have been pursued to improve the plasticity of this type of alloys. For example, annealing treatments at intermediate temperatures, i.e., between the glass transition temperature (T_g) and the crystallization temperature (T_X), can result in a certain increase of plastic strain,[32] as well as a increase of hardness.[33] However, different (and sometimes contrasting) effects are often observed after annealing depending on the exact alloy composition and the heat treatment conditions. For example, apart from causing nucleation and growth of nanocrystals, the annealing process usually affects also the amorphous matrix in different ways. First, since the nanocrystals typically have a different composition from that of the matrix, the composition of the matrix will change as well, sometimes resulting in a different overall mechanical behavior. Another consideration is that the annealing process (often carried out above the glass transition temperature (T_g)) will change the state of structural relaxation of the matrix, causing a reduction of free volume that can be expressed as a change in the fictive temperature of the glass.[34,35] Usually, a reduction in free volume due to structural relaxation leads to embrittlement of the glass.[36,37]

The minor addition is an effective way for enhanced mechanical properties, as well as for improved the GFA and corrosion resistance of the Ti-based glassy alloys. The minor addition is fundamental to controlling the formation, manufacture and properties of materials because the nucleation of crystalline phases is relevant for all solidification and the minor addition is an effective way to control the nucleation.

Addition of Sn is helpful in term of glass formation and improving the thermal stability for Ti-based glassy alloys.[38,39] Substitution of Cu by 2 at% Sn in a $Ti_{40}Zr_{10}Cu_{36}Pd_{14}$ glassy alloy increased the plasticity (around 3%) without compromising the strength,[38] also improved significantly the GFA of the resulting alloy.[39] The $Ti_{40}Zr_{10}Cu_{34}Pd_{14}Sn_2$ bulk glassy alloy rod with a diameter of 12 mm has been fabricated by copper mold casting technique (Fig. 4). The additions of 2∼4 at% Sn enlarged the supercooled liquid region, indicating good thermal stability. Ti–Zr–Cu–Pd–Sn bulk glassy alloys exhibited high compressive strength of about 2000–2050 MPa.[39] Moreover, the Ti–Zr–Cu–Pd–Sn bulk glassy alloys also exhibited a higher corrosion resistance and lower passive current density than those of pure Ti and Ti–6Al–4V alloy when they were immersed in NaCl, H_2SO_4, lactic acid, PBS (phosphate-buffered saline without calcium and magnesium salts solution) and HBSS (Hanks' balance salt solution without calcium, magnesium and phenol red), respectively, at 310 K.[40–42]

Minor additions of noble elements such as Au and Pt also improved significantly plastic stain of the Ti–Zr–Cu–Pd glassy alloys (Fig. 5), due to nano-particles dispersed in the glassy matrix blocking the propagation of shear bands.[43] High yield strength of about 2000 MPa, low Young's modulus of about 80 GPa and distinct plastic strain of about 1.5–10% were achieved in 1% noble element-added alloys. In addition, only 1 at% Si addition was effective in facilitating glass formation for the Ti-based glassy alloys,[24,44] and minor Si addition was favor of enlarging the super liquid region (SCL).[24,45,46]

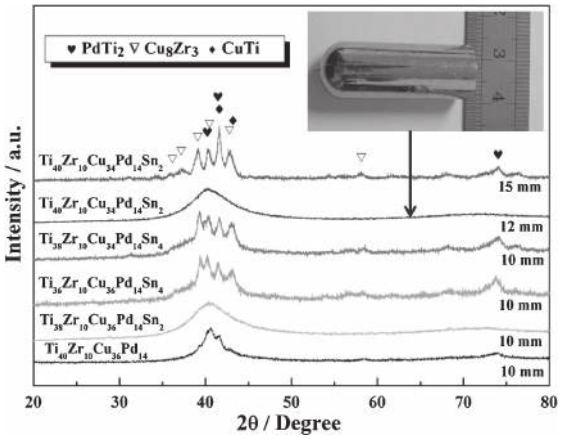

Fig. 4 XRD patterns of TiZrCuPdSn bulk glassy alloys.[39)]

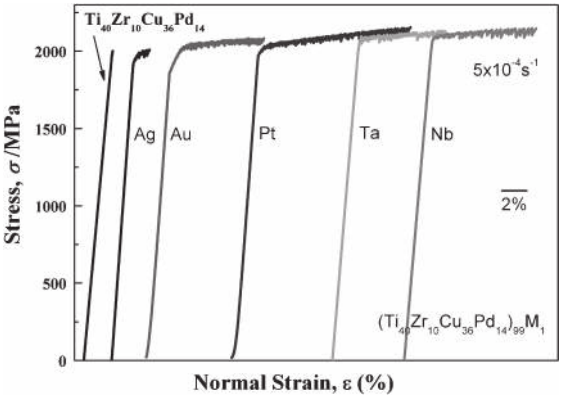

Fig. 5 Compressive stress–strain curves of the $(Ti_{40}Zr_{10}Cu_{36}Pd_{14})_{99}M_1$ alloys.

The most convenient element to be added to Ti–Zr–Cu–Pd glassy alloys has been shown to be Nb.[47–50)] This element is tougher than Sn, it is biocompatible, and it can enhance the plasticity of BMGs by (1) *in-situ* formation of ductile bcc phase,[51,52)] (2) formation of quasi-crystals[53)] or medium range ordered (MRO) clusters[54)] and (3) nano-particles embedded in the glassy matrix.[47)] High strength and distinct plastic strain were observed in the stress–strain curves for Nb-added Ti–Zr–Cu–Pd alloys. In particular, yield strength exceeding 2050 MPa, low Young's modulus of about 80 GPa and distinct plastic strain of 6.5 and 8.5% corresponding to serrated flow sections are obtained in the 1% (Fig. 5) and 3% Nb-added alloys, respectively.[47)] The additions of the minor Nb or Ta also exhibit higher corrosion resistance,[55)] as shown in Fig. 6.

2.3 Large-size Ti-based metallic glasses and the composites by powder metallurgy

It is well known that the BMGs are commonly produced by using two kinds of production techniques of solidification such as copper mould casting, water quenching, etc., and consolidation. However, using solidification technique, a rather high cooling rate is required to suppress the formation of more thermodynamically stable crystalline phases. Sample size and shape are seriously limited, thereby limiting the range of their applications. On the other hand, using consolidation technique, it is possible to produce larger

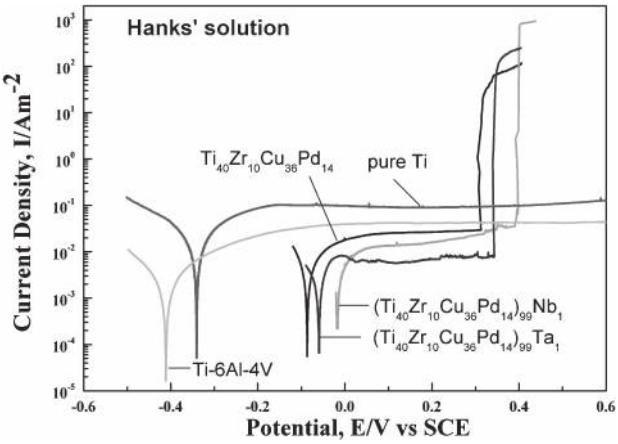

Fig. 6 Potentiodynamic polarization curves of the $(Ti_{40}Zr_{10}Cu_{36}Pd_{14})_{99}M_1$ alloys immersed in Hanks' solution at 310 K. The curves of pure Ti and Ti–6Al–4V alloy are also shown for comparison.

metallic glassy alloy parts in a variety of shapes than those fabricated by solidification technique. Spark plasma sintering (SPS) process, as a rapid consolidation technique,[56–60)] has a great potential for consolidating amorphous materials. Using the SPS process, large-size Zr-based,[61–66)] Cu-based,[67–71)] Ni-based,[72–77)] Fe-based[78–80)] and Mg-based[81)] BMGs and their composites have been developed.

Recently, large size and high strength Ti-based BMGs and their composites have been developed by the spark plasma sintering of the gas-atomized Ti-based glassy powders, or the mixed powders blended with crystalline powders.[82–88)] Ni- and Be-free Ti-based ($Ti_{45}Zr_{10}Cu_{31}Pd_{10}Sn_4$) atomized glassy powder was consolidated by the SPS process at various sintering temperatures. The samples sintered by the SPS process at a sintering temperature of 643 K with a loading pressure of 600 MPa exhibited high strength, high densification and a full glassy structure, and the potentiodynamic polarization curve showed a flat passive region after active dissolution at open-circuit potential, having a higher pitting potential.[82)] The fractured strength of the sample sintered at 643 K was 2060 MPa, which is similar to that of the casting sample of the $Ti_{45}Zr_{10}Cu_{31}Pd_{10}Sn_4$ glassy alloy.[40)]

As the candidate for implants, the biocompatibility of Ti-based bulk glassy alloys should be considered. Hydroxyapatite (HA), which is a main mineral constituent of teeth and bone, has an excellent biocompatibility with hard tissue, skin and muscle tissue. Moreover, HA does not exhibit any cytoxic effects and can directly bond to human bone.[89–91)] A number of studies have been reported on HA coating on Ti metal and Ti-alloys for improving the surface bioactivity.[92–95)] However, the HA coatings of metallic implants often flake off as a result of poor ceramic/metal interface bonding, which may cause surgery to fail.[96)] This problem may be solved by fabrication of metal/HA composites.

Using the mixed powders of the gas-atomized Ti-based glassy powder blended with the HA powder having various contents, large size and high strength Ti-based glassy matrix composites have been developed by the SPS process.[84–87)] Figure 7 shows the optical microscopy images of Ti-based ($Ti_{40}Zr_{10}Cu_{36}Pd_{14}$) glassy alloy/HA composites.[86)] For the

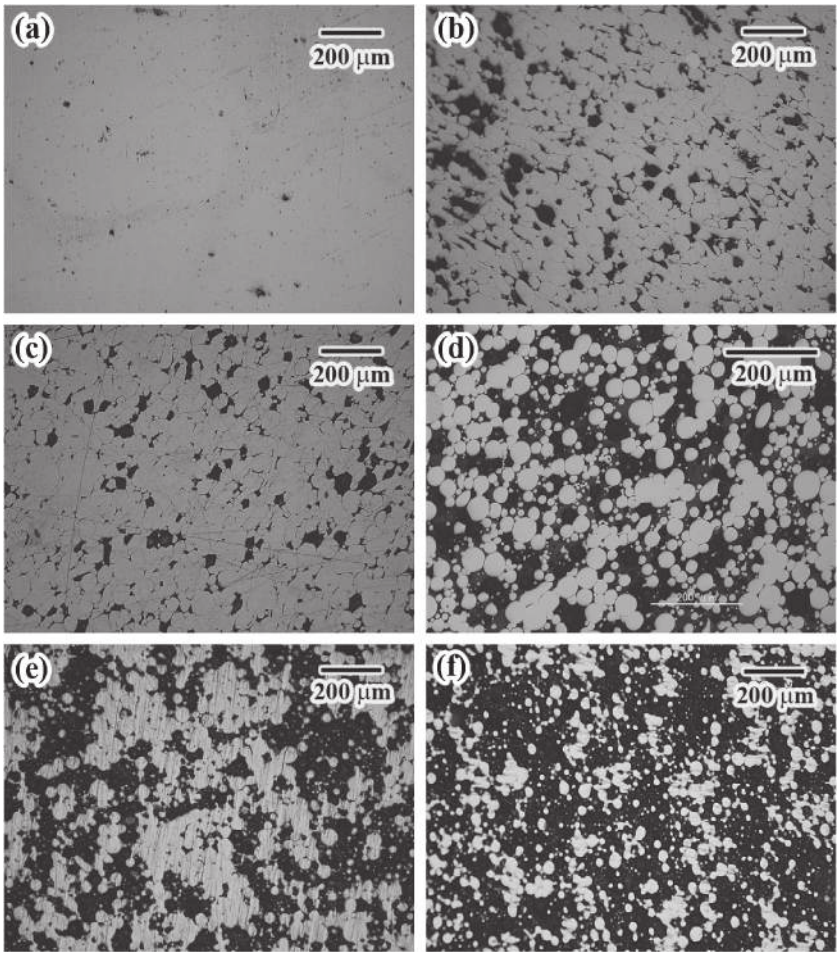

Fig. 7 Microstructures of the Ti-based ($Ti_{40}Zr_{10}Cu_{36}Pd_{14}$) glassy composites with different HA contents sintered by the SPS process at 643 K, 600 MPa, 10 min. (a) 0; (b) 1 mass%; (c) 2 mass%; (d) 3 mass%; (e) 5 mass%; and (f) 10 mass%.[86]

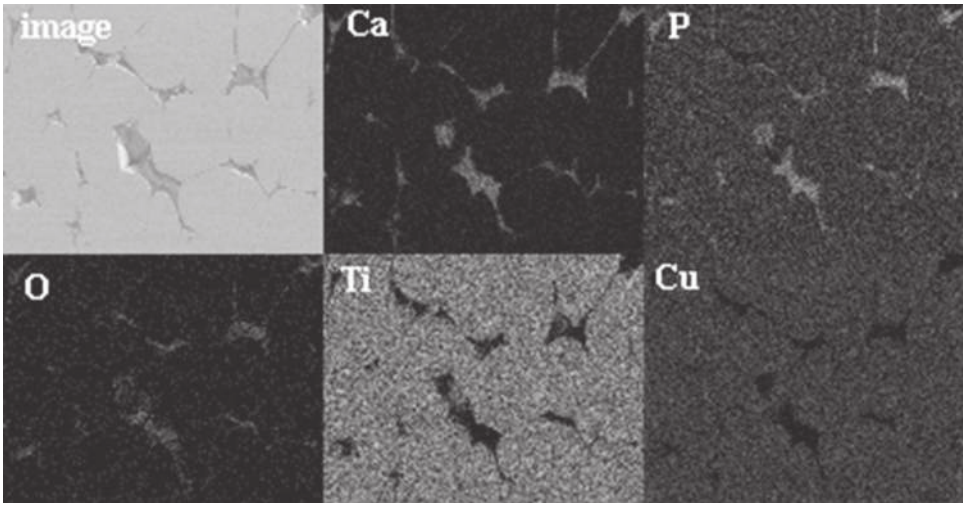

Fig. 8 Element mapping patterns of the Ti-based ($Ti_{40}Zr_{10}Cu_{36}Pd_{14}$) glassy composite with 2 mass% HA addition sintered by the SPS process at 643 K, 600 MPa, 10 min.[87]

sample without HA, $Ti_{40}Zr_{10}Cu_{36}Pd_{14}$ powders are coalesced by the neck formation. No obvious interface is observed between glassy powders. Some small pores (less than 10 μm) in the coalesced powders are seen (Fig. 7(a)). For the samples with 1 or 2 mass% HA additions, $Ti_{40}Zr_{10}Cu_{36}Pd_{14}$ glassy alloy powders are also coalesced and HA particles are homogeneously distributed over the entire sintered sample, as shown in Figs. 7(b) and 7(c). Figure 8 presents the corresponding two-dimensional mapping patterns of the elements of Ca, P, O, Ti and Cu for the sintered composite sample with a HA content of 2 mass%.[87] It is seen that the HA particles are in a polyhedral shape, and distribute in the

whole sintered samples. Because the HA has a poor strength (lower than 150 MPa),[91] the HA particles are crushed and filled in the residual space among the Ti-based glassy powders due to the high applied loading pressure of 600 MPa. Furthermore, significant deformation of Ti-based glassy powders is also observed, as shown in Fig. 7. This is due to the viscous flow which can occur at the sintering temperature. With increasing the HA content to over 3 mass%, distribution of the HA particles became inhomogeneous, and partial crystallization was caused. The strength decreased with increase of the HA content.[86] On the other hand, the Ti-based glassy alloy/HA composites usually showed poor fracture toughness; it was difficult to perform tensile test of the composites.

2.4 Porous Ni- and Be-free Ti-based metallic glasses by powder metallurgy

Developments of the large size and high strength Ti-based BMGs without toxic and allergic elements make it possible to create BMG implants. However, one of major problems concerning metallic implants in orthopedic surgery is mismatch of Young's modulus between bone (10–30 GPa)[1] and metallic implants (about 82 GPa for $Ti_{40}Zr_{10}Cu_{36}Pd_{14}$ glassy alloy).[30] Bone is insufficiently loaded due to the mismatch, which is called "stress-shielding".[97] One way to overcome the problem is to reduce Young's modulus of metallic implants by introducing pores.

Oh *et al.*[98] reported that the porous Ti having Young's modulus comparable to the human bone was fabricated by hot-pressing method, while the strength was lower than that of bone. By spark plasma sintered the mixture of the gas-atomized Ti-based glassy alloy powders and solid salt (NaCl) powders, followed by leaching treatment into water to eliminate the salt phase, high strength porous Ti-based BMGs (Fig. 9) with low Young's modulus, which is comparable to that of bone, were produced.[99] The pores are homogeneously distributed in the whole sintered samples. The porosity can be controlled by controlling the volume fraction of the adding salt phase. Corrosion behavior of the porous Ti-based BMGs has been investigated by polarization process in Hanks' solution. Figure 10 shows the potentiodynamic polarization curves of the porous Ti-based BMG samples in Hanks' solution at 310 K.[99] The porous Ti-based BMG alloys exhibit about 300 mV higher open-circuit potential than that of pure Ti. The porous sample with a porosity of 50% presents a similar corrosion behavior as that of 60% alloy. The anodic current density between 10^{-3} and 10^{-1} Am^{-2} is more than one order of magnitude lower than that of the pure Ti. However, the passivation range is much narrow than that of pure Ti, indicating the more susceptibility of the pitting corrosion. The anodic current density in the porous Ti-based BMGs slowly increases during anodic polarization, suggesting the crevice corrosion mechanism. Furthermore, using a Ti-based metallic glassy/nanocrystalline powders prepared by gas-atomization method,[100] Wang *et al.*[101] produced porous Ti-based metallic glassy/nanocrystalline composites by the SPS process. The sintered composite samples exhibited high fracture strength ranging from 400 to 730 MPa corresponding with the porosity of about 25 and 15%, respectively.

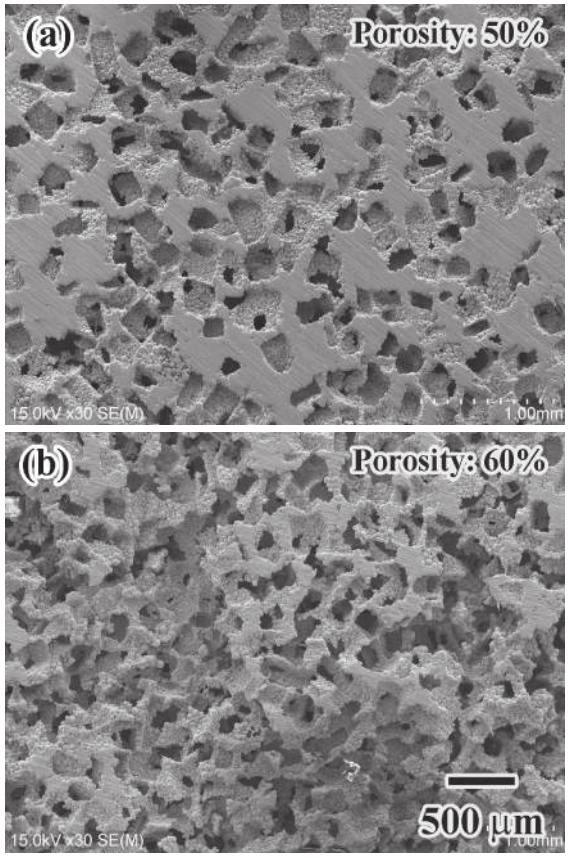

Fig. 9 SEM images of the cross section of the produced porous $Ti_{45}Zr_{10}Cu_{31}Pd_{10}Sn_4$ BMG samples after leaching the salt phase with the porosity of 50% (a) and 60% (b). The images were taken from the centre area of the samples.[99]

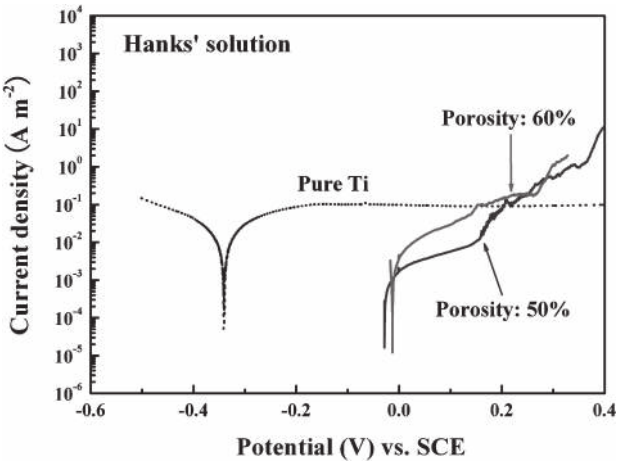

Fig. 10 Potentiodynamic polarization curves of the produced porous $Ti_{45}Zr_{10}Cu_{31}Pd_{10}Sn_4$ BMG samples by the SPS process with various porosities in Hanks' solution at 310 K. The curve of pure Ti is also shown for comparison.[99]

3. Bioactivity and *In Vivo* Evaluations of Ti-Based Metallic Glasses

3.1 Surface treatment and bioactivity

It is known that the bioactivity of metallic implants is usually evaluated by the nucleation and growth of hydroxyapatite. However, recent results have demonstrated that

hydroxyapatite can't be formed on the surface of Ti-based BMGs after simple immersion in 5 M NaOH solution followed by immersion in simulated body fluid (SBF).[102] Some apatite particles were deposited only physically and covered on the surface of Ti-based BMGs with hydrothermal hot-pressing treatment.[103] The formation and growth rate of bone-like apatite on metallic implants in SBF before implant are usually regarded as a criterion in evaluating bioactivity of metallic implants. Therefore, the most important factor before the Ti-based BMGs are implanted is to succeed in growing bone-like apatite or similar calcium phosphate layer on Ti-based BMGs.

Hydroxyapatite coatings have been developed as a chemical bonding between metallic implants and the host bone tissue implanted because hydroxyapatite is mineral and chemically similar to bone. Many coating or surface modification technologies, such as thermal decomposition,[104] sputtering[105,106] and micro-arc oxidation,[107,108] have been developed to enhance the bioactivity (bone-bonding ability) of Ti alloy implants. However, these techniques require high-temperature or high-vacuum conditions that cause cracks in the fabricated films during cooling. For coating or surface modification of BMGs, low-temperature processes such as chemical treatment are more desirable as such processes maintain their excellent mechanical properties. If not, these BMGs will crystallize, resulting in degradation of their properties. In general, a simple chemical and thermal two-step treatment method is widely used to conventional Ti alloys because the bone-like apatite can be formed in biomimetic solution.[109,110] However effect of this method is limited to the Ti-based BMGs.

In order to improve apatite-forming ability of Ti-based BMGs, some methods such as Ti coating on Ti-based BMG substrates by physical vapor deposition (PVD) technique,[102,111] and a two-step method consisting of hydrothermal-electrochemical treatment followed by pre-calcification treatment,[112] have been developed.

The $Ti_{40}Zr_{10}Cu_{36}Pd_{14}$ BMG samples were coated by a PVD method using magnetron-sputtering of pure Ti metal cathode in a nitrogen protective atmosphere at 473 K, then were treated in 5 M NaOH solution at 333 K for 24 h, which was demonstrated that sodium titanate layer with a porous structure was formed on the surface of the Ti-coated $Ti_{40}Zr_{10}Cu_{36}Pd_{14}$ BMGs. A bone-like hydroxyapatite layer was formed on the alkali-treated Ti-coated $Ti_{40}Zr_{10}Cu_{36}Pd_{14}$ BMGs after a short-time immersion in simulated body fluid (SBF).[102] After the samples were immersed only for one day, a few white nuclei were observed, demonstrating that the initiation of nucleation was fulfilled within a short immersion time. With an increase of the immersion time, the particles gradually proliferated and spread all over the surface during a 15-day immersion. Figure 11(a) shows a scanning electron microscopy (SEM) cross-section image of Ti-coated $Ti_{40}Zr_{10}Cu_{36}Pd_{14}$ BMG after a 15-day immersion in SBF.[102] The thickness of calcium phosphate layer is about 300 nm. The porous hydroxyapatite shows a good bonding with the previously alkali-treated layer. Figure 11(b) shows the X-ray diffractometry (XRD) pattern of the surface of the Ti-coated $Ti_{40}Zr_{10}Cu_{36}Pd_{14}$ BMG after immersion in SBF for 15 days.[102] The characteristic peaks arising from hydroxyapatite

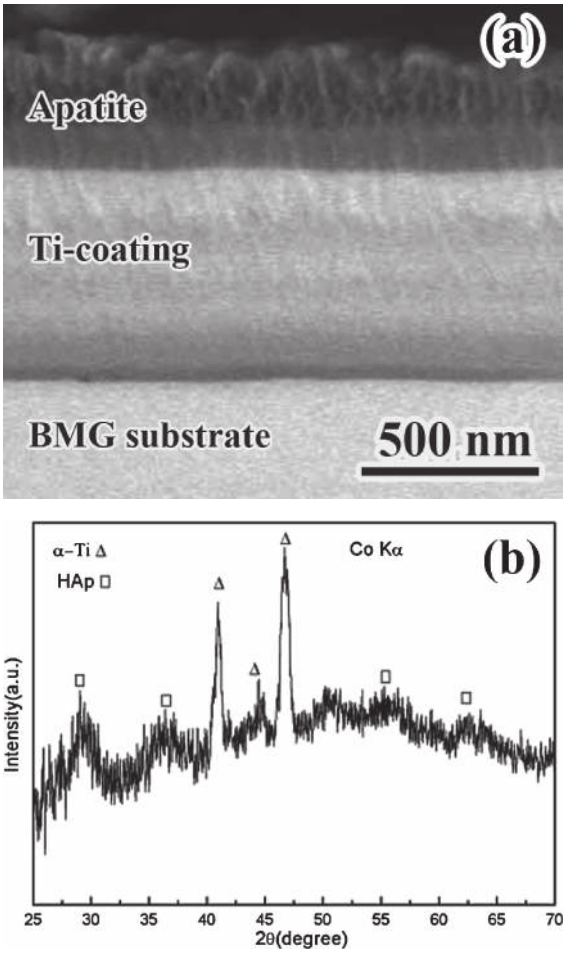

Fig. 11 SEM cross-section morphology (a) and the surface XRD pattern (b) of alkali-treated Ti-coated $Ti_{40}Zr_{10}Cu_{36}Pd_{14}$ BMG immersed in Hanks' solution for 15 days.

as well as some peaks from α-Ti are identified. The corresponding X-ray energy dispersive spectroscopy (EDS) analysis results demonstrated that the surface particles were rich in Ca and P, with a Ca/P ratio being about 1.6, which is similar to the ratio of hydroxyapatite.

Recently, a low-temperature two-step treatment method developed by Yoshimura *et al.*[112] for fabricating a crack-free titanate coating on Ti metal and alloys have also been applied to prepare a bioactive surface on the Ti-based metallic glasses.[113–116] The two-step treatment consists of hydrothermal-electrochemical treatment followed by pre-calcification treatment. After hydrothermal-electrochemical treatment of a Ti-based ($Ti_{40}Zr_{10}Cu_{36}Pd_{14}$) metallic glass sample, a micro-porous and network structure is formed on the surface of the glassy alloy, as shown in Fig. 12(a).[116] A grown composite layer named as "graded intermediated layer" or "growing integrated layer (GIL)"[117] with a thickness of several hundred nanometers is formed in the hydrothermal-electrochemical treated $Ti_{40}Zr_{10}Cu_{36}Pd_{14}$ metallic glass, as shown in Fig. 12(b).[116] The outer layer (Layer 1 in Fig. 12(b)) is the porous and network layer formed by the reaction of the alloy components with the alkali solution. The inner layer (Layer 2 in Fig. 12(b)) is the intermediated layer lying between the metallic glass substrate (Layer 3) and the outer porous layer, which is formed by elemental

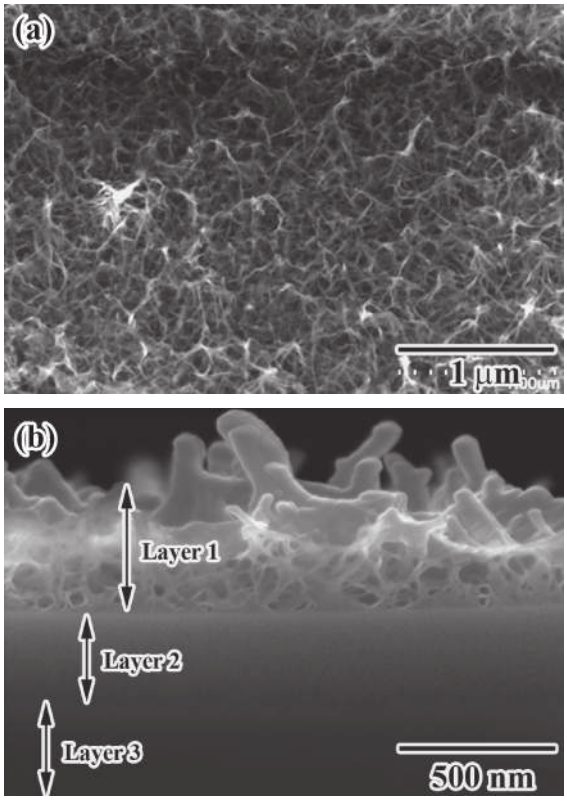

Fig. 12 SEM images of $Ti_{40}Zr_{10}Cu_{36}Pd_{14}$ metallic glass after electrochemical-hydrothermal treatment in 1 M NaOH solution. (a) Surface morphology and (b) cross section morphology.[116)]

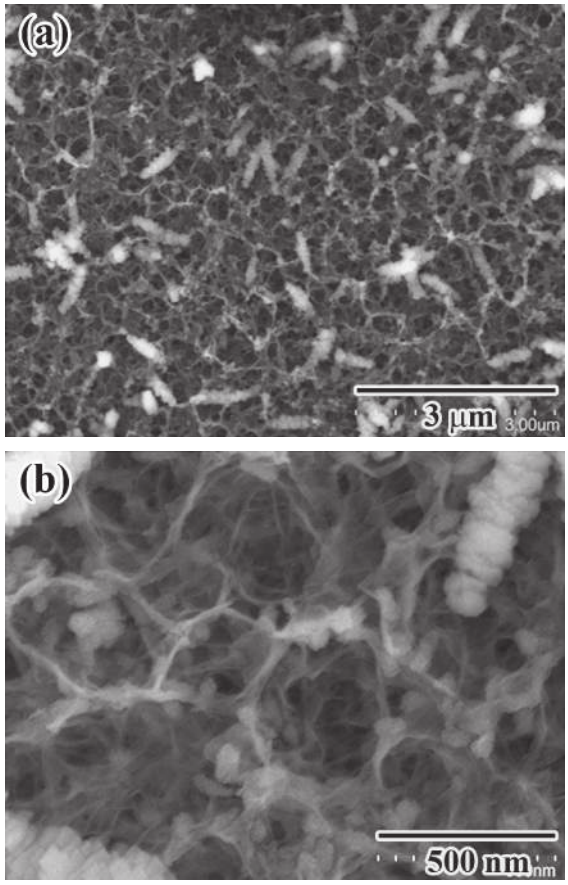

Fig. 13 SEM images of electrochemical-hydrothermal treated $Ti_{40}Zr_{10}Cu_{36}Pd_{14}$ metallic glass after pre-calcification treatment. (a) Low magnification (b) high magnification.[116)]

diffusion to the outer layer. After pre-calcification treatment for the glassy samples treated by hydrothermal-electrochemical process, some white claviform nuclei distribute on the surface of the samples, as shown in Fig. 13.[116)] The sizes of nuclei are about 1 μm in length, and enriched with Ca and P elements analyzed by EDS. Under high magnification, some smaller white granules can also be observed, as shown in Fig. 13(b). Both HPO_4^- and Ca^{2+} ions could be absorbed into the microporous titania surface, which is expected to stimulate the nucleation and growth of calcium phosphate during immersion in Hanks' solution. After the two-step pretreatment, the samples were immersed in Hanks' solution at 310 K with different times. After immersion of one day, a thin and homogeneous layer appears in the network surface (Fig. 14(a)),[116)] which is composed of Ca, P and O. The Ca/P ratio is identified to be 1.3 by EDS. Then the layer grows and the Ca content increases with an increase in immersion time. With further increasing time to six days, the Ca/P ratio reaches about 1.6, which is similar to the ratio of apatite. Figure 15(a) shows the cross section SEM image of the two-step treated $Ti_{40}Zr_{10}Cu_{36}Pd_{14}$ metallic glass after immersion in Hanks' solution for six days.[116)] The porous apatite (Layer 1 in Fig. 15(a)) is strongly bonded with the porous surface (Layer 2 in Fig. 15(a)) of the metallic glass. The thickness of the resulting apatite is about several hundred nanometers. Figure 15(b) shows elemental depth profiles by Auger electron spectroscopy (AES) of the pretreated Ti-based metallic glass after immersion in Hanks' solution for six days.[116)] The surface layer (Layer 1 in Fig. 15(b)) consists mainly of Ca, P and O elements.

3.2 Osteoblast response

The success of an implant is determined by its integration into the tissue surrounding the material. Cell adhesion and cell spreading is an important parameter for implant engineering. Oak *et al.*[118)] carried out a series of studies about the corrosion behavior and biocompatibility of the $Ti_{45}Zr_{10}Cu_{31}Pd_{10}Sn_4$ metallic glass, and their results demonstrated that this kind of metallic glass exhibited good corrosion resistance and excellent biocompatibility in osteoblast culture test. Nagai *et al.*[119)] investigated cellular behaviors responding to the Ti-based ($Ti_{40}Zr_{10}Cu_{36}Pd_{14}$) metallic glass surface irradiated with a femtosecond laser,[120)] which can form periodic nanostructures on the Ti-based BMG surface.[121)] The results demonstrated that the number of osterblasts attached to the modified Ti-based metallic glass surfaces after 3 h of incubation. Li *et al.*[122)] evaluated the effect of the surface roughness of Ti-based BMGs on the osteoblast responses. Surfaces with different roughness were prepared by sand blasting using corundum with various grit sizes. The corundum sand blasting surfaces significantly increased the surface wettability and cell attachment, cell proliferation, and alkaline phosphatase (ALP) activity. The sample surface treated by large grit corundum was more favorable for cell attachment, proliferation, and differentiation than samples treated by small grit corundum.

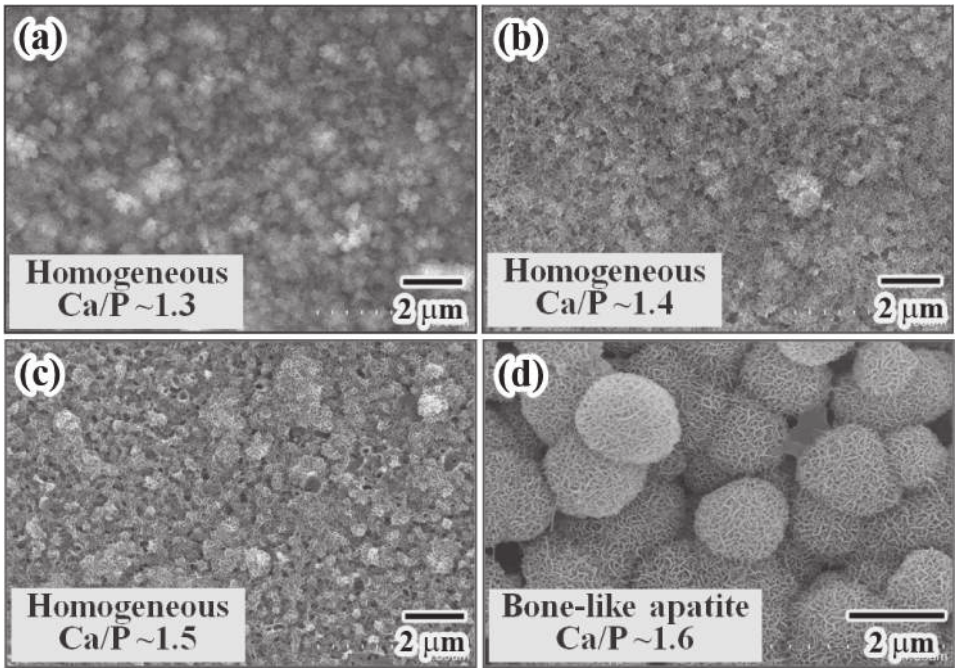

Fig. 14 SEM images of two-step pretreated $Ti_{40}Zr_{10}Cu_{36}Pd_{14}$ metallic glass after immersion in Hanks' solution at 310 K for different times (a) one (b) two (c) three and (d) six days.[116]

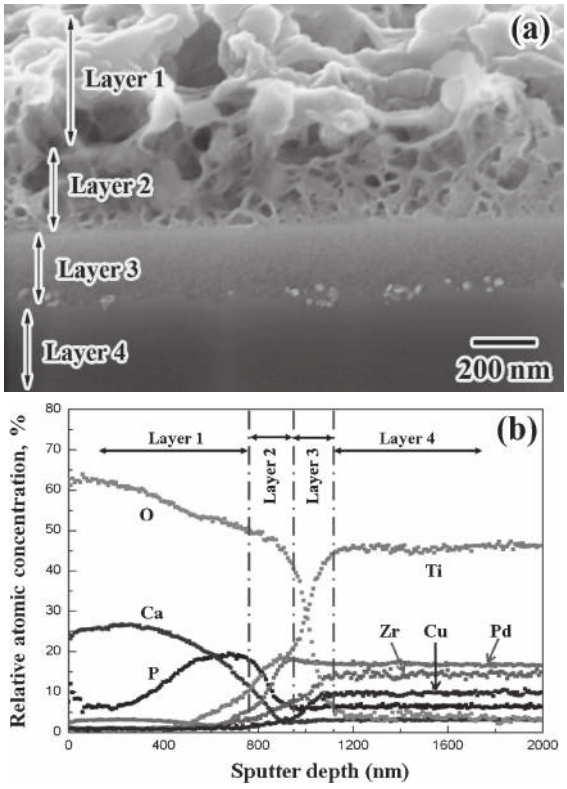

Fig. 15 Cross sectional SEM image (a) and elemental depth profiles by Auger electron spectroscopy (b) of two-step treated $Ti_{40}Zr_{10}Cu_{36}Pd_{14}$ metallic glass after immersion in Hanks' solution at 310 K for six days.

3.3 *In vivo* tests

By implanting the Ti-based ($Ti_{40}Zr_{10}Cu_{34}Pd_{14}Sn_2$) BMG rods in the back subcutaneously and in the femoral condyle of rats, *in vivo* evaluation of its biocompatibilities has been carried out.[123] There was no obvious inflammatory reaction or foreign body response occurred around the implanted Ti-based glassy alloy bars. No hyperemia or edema was found in either subcutaneous or bone tissue. The subcutaneous samples showed mild capsule reaction of fibroblasts without inflammatory cells invasion. Toluidine blue section of bone samples showed that new bone regenerated directly on the metallic glass surface and covered it in whole circumference. EDS scan detected no metal ion diffusion locally. Ti-based BMG bars displayed excellent biocompatibility in both soft tissue and hard tissue, it also showed excellent osteoconductivity when implanted in bone tissue and no metal ion diffusion was found up to one month after operation. The Ti-based BMGs should be a strong candidate for the clinic applications that require mechanical strength highly.

4. Conclusions

Ti-based (Ti–Zr–Cu–Pd) BMGs without toxic and allergic elements have been developed. Minor additions of Nb, Ta, Sn, Au, Pt, etc. are demonstrated to be effective on improved mechanical properties, enhanced GFA and corrosion resistance of the Ti–Zr–Cu–Pd BMGs. Using the SPS process, large-size and high strength Ti-based BMGs and the composites, as well as porous Ti-based glassy alloys having approximate Young's modulus with that of bone have been developed. These glassy alloys and the composites exhibit high strength, low Young's modulus, large plasticity, good corrosion resistance and excellent biocompatibility. After a two-step treatment (hydrothermal-electrochemical treatment followed by pre-calcification treatment), a bioactive surface is formed on the Ti-based metallic glasses. These excellent properties make the Ti-based BMGs become competent candidate for application as biomaterials.

Acknowledgements

The work was supported by Grant-In-Aid for Science Research in a Priority Area on "Research and Development Project on Advanced Materials Development and Integration of Novel Structured Metallic and Inorganic Materials" from the Ministry of Education, Sports, Culture, Science and Technology, Japan.

REFERENCES

1) M. Long and H. J. Rack: Biomaterials **19** (1998) 1621–1639.
2) K. Wang: Mater. Sci. Eng. A **213** (1996) 134–137.
3) M. Geetha, A. K. Singh, R. Asokamani and A. K. Gogia: Prog. Mater. Sci. **54** (2009) 397–425.
4) M. Niinomi: Metall. Mater. Trans. A **33** (2002) 477–486.
5) A. Inoue and A. Takeuchi: Acta Mater. **59** (2011) 2243–2267.
6) A. Inoue: Acta Mater. **48** (2000) 279–306.
7) W. L. Johnson: MRS Bull. **24** (1999) 42–56.
8) T. Zhang, A. Inoue and T. Masumoto: Mater. Sci. Eng. A **181–182** (1994) 1423–1426.
9) A. Inoue, N. Nishiyama, K. Amiya, T. Zhang and T. Masumoto: Mater. Lett. **19** (1994) 131–135.
10) T. Zhang and A. Inoue: Mater. Trans. JIM **39** (1998) 1001–1006.
11) T. Zhang and A. Inoue: Mater. Trans. **40** (1999) 301–306.
12) T. Zhang and A. Inoue: Mater. Sci. Eng. A **304–306** (2001) 771–774.
13) Y. H. Kim, W. T. Kim and D. H. Kim: Mater. Trans. **43** (2002) 1243–1246.
14) Y. C. Kim, D. H. Bae, W. T. Kim and D. H. Kim: J. Non-Cryst. Solids **325** (2003) 242–250.
15) C. L. Ma, S. Ishihara, H. Soejima, N. Nishiyama and A. Inoue: Mater. Trans. **45** (2004) 1802–1806.
16) M. X. Xia, C. L. Ma, H. X. Zheng and J. G. Li: Mater. Sci. Eng. A **390** (2005) 372–375.
17) Y. J. Huang, J. Shen, J. F. Sun and X. B. Yu: J. Alloy. Compd. **427** (2007) 171–175.
18) Y. C. Kim, J. M. Park, J. K. Lee, D. H. Bae, W. T. Kim and D. H. Kim: Mater. Sci. Eng. A **375–377** (2004) 749–753.
19) Y. C. Kim, W. T. Kim and D. H. Kim: Mater. Sci. Eng. A **375–377** (2004) 127–135.
20) J. M. Park, Y. C. Kim, W. T. Kim and D. H. Kim: Mater. Trans. **45** (2004) 595–598.
21) G. Duan, A. Wiest, M. L. Lind, A. Kahl and W. L. Johnson: Scr. Mater. **58** (2008) 465–468.
22) K. Amiya, N. Nishiyama, A. Inoue and T. Masumoto: Mater. Sci. Eng. A **179–180** (1994) 692–696.
23) X. H. Lin and W. L. Johnson: J. Appl. Phys. **78** (1995) 6514–6519.
24) C. L. Ma, H. Soejima, S. Ishihara, K. Amiya, N. Nishiyama and A. Inoue: Mater. Trans. **45** (2004) 3223–3227.
25) F. X. Qin, X. M. Wang, A. Kawashima, S. L. Zhu, H. Kimura and A. Inoue: Mater. Trans. **47** (2006) 1934–1937.
26) A. Inoue, T. Zhang and T. Masumoto: J. Non-Cryst. Solids **156–158** (1993) 473–480.
27) A. Inoue: Mater. Trans. JIM **36** (1995) 866–875.
28) A. Inoue: Mater. Sci. Eng. A **226–228** (1997) 357–363.
29) S. L. Zhu, X. M. Wang, F. X. Qin, M. Yoshimura and A. Inoue: Mater. Trans. **48** (2007) 2445–2448.
30) S. L. Zhu, X. M. Wang, F. X. Qin and A. Inoue: Mater. Sci. Eng. A **459** (2007) 233–237.
31) F. X. Qin, M. Yoshimura, X. M. Wang, S. L. Zhu, A. Kawashima, K. Asami and A. Inoue: Mater. Trans. **48** (2007) 1855–1858.
32) F. X. Qin, X. M. Wang and A. Inoue: Intermetallics **15** (2007) 1337–1342.
33) J. Fornell, N. V. Steenberge, A. Varea, E. Rossinyol, E. Pellicer, S. Suriñach, M. D. Baró and J. Sort: J. Mech. Behav. Biomed. Mater. **4** (2011) 1709–1717.
34) T. Egami: Intermetallics **14** (2006) 882–887.
35) C. A. Schuh, T. C. Hufnagel and U. Ramamurty: Acta Mater. **55** (2007) 4067–4109.
36) T. W. Wu and F. Spaepen: Philos. Mag. B **61** (1990) 739–750.
37) P. Lamparter and S. Steeb: J. Non-Cryst. Solids **106** (1988) 137–146.
38) S. L. Zhu, X. M. Wang and A. Inoue: Intermetallics **16** (2008) 1031–1035.
39) S. L. Zhu, G. Q. Xie, F. X. Qin, X. M. Wang and A. Inoue: Mater. Trans. **53** (2012) 500–503.
40) J. J. Oak, D. V. Louzguine-Luzgin and A. Inoue: J. Mater. Res. **22** (2007) 1346–1353.
41) C. L. Qin, J. J. Oak, N. Ohtsu, K. Asami and A. Inoue: Acta Mater. **55** (2007) 2057–2063.
42) J. J. Oak, D. V. Louzguine-Luzgin and A. Inoue: Mater. Sci. Eng. C **29** (2009) 322–327.
43) F. X. Qin, G. Q. Xie, Z. H. Dan and A. Inoue: Appl. Mech. Mater. **148–149** (2012) 241–244.
44) S. L. Zhu, X. M. Wang, F. X. Qin and A. Inoue: Mater. Trans. **48** (2007) 163–166.
45) S. L. Zhu, X. M. Wang, F. X. Qin, M. Yoshimura and A. Inoue: Intermetallics **16** (2008) 609–614.
46) S. L. Zhu, G. Q. Xie, F. X. Qin and X. M. Wang: Mater. Sci. Forum **750** (2013) 36–39.
47) F. X. Qin, X. M. Wang, G. Q. Xie and A. Inoue: Intermetallics **16** (2008) 1026–1030.
48) J. Fornell, E. Pellicer, N. V. Steenberge, S. González, A. Gebert, S. Suriñach, M. D. Baró and J. Sort: Mater. Sci. Eng. A **559** (2013) 159–164.
49) S. F. Shan, Z. J. Zhan, C. Z. Fan, Y. Z. Jia, B. Q. Zhang, R. P. Liu and W. K. Wang: Chin. Phys. Lett. **25** (2008) 4165–4167.
50) Z. Y. Suo, K. Q. Qiu, Q. F. Li, Y. L. Ren and Z. Q. Hu: Mater. Sci. Eng. A **527** (2010) 2486–2491.
51) G. He, J. Eckert, W. Loser and L. Schultz: Nat. Mater. **2** (2003) 33–37.
52) U. Kühn, N. Mattern, A. Gebert, M. Kuusy, U. Siegel and L. Schultz: Intermetallics **14** (2006) 978–981.
53) C. L. Qiu, L. Liu, M. Sun and S. M. Zhang: J. Biomed. Mater. Res. A **75A** (2005) 950–956.
54) J. M. Park, J. H. Na, D. H. Kim, K. B. Kim, N. Mattern, U. Kühn and J. Eckert: Philos. Mag. **90** (2010) 2619–2633.
55) F. X. Qin, G. Q. Xie, S. L. Zhu and Z. H. Dan: Mater. Sci. Forum **750** (2013) 23–26.
56) G. Q. Xie, O. Ohashi, T. Yoshioka, M. Song, K. Mitsuishi, H. Yasuda, K. Furuya and T. Noda: Mater. Trans. **42** (2001) 1846–1849.
57) G. Q. Xie, O. Ohashi, N. Yamaguchi and A. Wang: Metall. Mater. Trans. A **34** (2003) 2655–2661.
58) M. Omori: Mater. Sci. Eng. A **287** (2000) 183–188.
59) V. Mamedov: Powder Metall. **45** (2002) 322–328.
60) M. Tokita: Mater. Sci. Forum **308–311** (1999) 83–88.
61) G. Q. Xie, W. Zhang, D. V. Louzguine-Luzgin, H. Kimura and A. Inoue: Scr. Mater. **55** (2006) 687–690.
62) G. Q. Xie, D. V. Louzguine-Luzgin, H. Kimura and A. Inoue: Mater. Trans. **48** (2007) 158–162.
63) G. Q. Xie, W. Zhang, D. V. Louzguine-Luzgin, H. Kimura and A. Inoue: Mater. Trans. **48** (2007) 1589–1594.
64) G. Q. Xie, D. V. Louzguine-Luzgin, H. Kimura and A. Inoue: Mater. Trans. **48** (2007) 1600–1604.
65) G. Q. Xie, D. V. Louzguine-Luzgin, F. Wakai, H. Kimura and A. Inoue: Mater. Sci. Eng. B **148** (2008) 77–81.
66) Z. H. Chu, H. Kato, G. Q. Xie, G. Y. Yuan, C. Lu and W. J. Ding: Mater. Sci. Eng. A **560** (2013) 40–46.
67) T. S. Kim, J. K. Lee, H. J. Kim and J. C. Bae: Mater. Sci. Eng. A **402** (2005) 228–233.
68) C. K. Kim, S. Lee, S. Y. Shin and D. H. Kim: Mater. Sci. Eng. A **449–451** (2007) 924–928.
69) G. Q. Xie, D. V. Louzguine-Luzgin, M. Fukuhara, H. Kimura and A. Inoue: Intermetallics **18** (2010) 1973–1977.
70) G. Q. Xie, D. V. Louzguine-Luzgin, M. Fukuhara, H. Kimura and A. Inoue: Mater. Sci. Forum **654–656** (2010) 1086–1089.
71) Z. H. Chu, H. Kato, G. Q. Xie, G. Y. Yuan, W. J. Ding and A. Inoue: J. Non-Cryst. Solids **358** (2012) 1263–1267.
72) G. Q. Xie, D. V. Louzguine-Luzgin, H. Kimura and A. Inoue: Appl. Phys. Lett. **90** (2007) 241902.
73) G. Q. Xie, D. V. Louzguine-Luzgin, H. Kimura, A. Inoue and F. Wakai: Appl. Phys. Lett. **92** (2008) 121907.

74) G. Q. Xie, D. V. Louzguine-Luzgin, S. Li, H. Kimura and A. Inoue: Mater. Trans. **50** (2009) 1273–1278.
75) G. Q. Xie, D. V. Louzguine-Luzgin, S. Li, H. Kimura and A. Inoue: Intermetallics **17** (2009) 512–516.
76) G. Q. Xie, D. V. Louzguine-Luzgin and A. Inoue: J. Alloy. Compd. **483** (2009) 239–242.
77) G. Q. Xie, D. V. Louzguine-Luzgin, H. Kimura and A. Inoue: Intermetallics **18** (2010) 851–858.
78) B. L. Shen and A. Inoue: J. Mater. Res. **18** (2003) 2115–2121.
79) S. Ishihara, W. Zhang, H. Kimura, M. Omori and A. Inoue: Mater. Trans. **44** (2003) 138–143.
80) G. Q. Xie, H. Kimura, D. V. Louzguine-Luzgin, H. Men and A. Inoue: Intermetallics **20** (2012) 76–81.
81) F. O. Méar, G. Q. Xie, D. V. Louzguine-Luzgin and A. Inoue: Mater. Trans. **50** (2009) 588–591.
82) G. Q. Xie, F. X. Qin, S. L. Zhu and A. Inoue: Intermetallics **29** (2012) 99–103.
83) D. J. Wang, Y. J. Huang, J. Shen, Y. Q. Wu, H. Huang and J. Zou: Mater. Sci. Eng. A **527** (2010) 2662–2668.
84) S. L. Zhu, X. M. Wang, G. Q. Xie, F. X. Qin, M. Yoshimura and A. Inoue: Scr. Mater. **58** (2008) 287–290.
85) S. L. Zhu, X. M. Wang, M. Yoshimura and A. Inoue: Mater. Trans. **49** (2008) 502–505.
86) S. L. Zhu, X. J. Yang and Z. D. Cui: Intermetallics **19** (2011) 572–576.
87) G. Q. Xie, S. L. Zhu and F. X. Qin: Mater. Sci. Forum **750** (2013) 52–55.
88) S. L. Zhu, G. Q. Xie, F. X. Qin, X. M. Wang and T. Hanawa: Mater. Trans. **54** (2013), doi:10.2320/matertrans.MF201311.
89) L. L. Hench: J. Am. Ceram. Soc. **74** (1991) 1487–1510.
90) T. K. Chaki and P. E. Wang: J. Mater. Sci.: Mater. Med. **5** (1994) 533–542.
91) R. Halouani, D. Bernache-Assloant, E. Champion and A. Ababou: J. Mater. Sci.: Mater. Med. **5** (1994) 563–568.
92) M. F. Chen, X. J. Yang, Y. Liu, S. L. Zhu, Z. D. Cui and H. C. Man: Surf. Coat. Technol. **173** (2003) 229–234.
93) X. J. Yang, R. X. Hu, S. L. Zhu, C. Y. Li, M. F. Chen, L. Y. Zhang and Z. D. Cui: Scr. Mater. **54** (2006) 1457–1462.
94) J. M. Choi, H. E. Kim and I. S. Lee: Biomaterials **21** (2000) 469–473.
95) A. Montenero, G. Gnappi, F. Ferrari, M. Cesari, E. Salvioli, L. Mattogno, S. Kaciulis and M. Fini: J. Mater. Sci. **35** (2000) 2791–2797.
96) C. Y. Yang, B. C. Wang, E. Chang and B. C. Wu: J. Mater. Sci. Mater. Med. **6** (1995) 258–265.
97) D. R. Sumner and J. O. Galante: Clin. Orthop. Relat. Res. **274** (1992) 202–212.
98) I. H. Oh, N. Nomura, N. Masahashi and S. Hanada: Scr. Mater. **49** (2003) 1197–1202.
99) G. Q. Xie, F. X. Qin, S. L. Zhu and D. V. Louzguine-Lugzin: Intermetallics (2013), submitted.
100) D. J. Wang, Y. J. Huang, J. Shen, Y. Q. Wu, H. Huang and J. Zou: Mater. Sci. Eng. A **527** (2010) 5750–5754.
101) D. J. Wang, Y. J. Huang, L. Z. Wu and J. Shen: Mater. Des. **44** (2013) 69–73.
102) F. X. Qin, X. M. Wang, T. Wada, G. Q. Xie, K. Asami and A. Inoue: Mater. Trans. **50** (2009) 605–609.
103) T. Onoki, X. M. Wang, S. L. Zhu, Y. Hoshikawa, N. Sugiyama, M. Akao, E. Yasuda, M. Yoshimura and A. Inoue: J. Ceram. Soc. Jpn. **116** (2008) 115–117.
104) P. Zhou and M. Akao: Biomed. Mater. Eng. **7** (1997) 67–81.
105) N. Ohtsu, K. Sato, A. Yanagawa, K. Saito, Y. Imai, T. Kohgo, A. Yokoyama, K. Asami and T. Hanawa: J. Biomed. Mater. Res. A **82A** (2007) 304–315.
106) K. Ueda, T. Narushima, T. Goto, M. Taira and T. Katsube: Biomed. Mater. **2** (2007) S160–S166.
107) M. S. Kim, J. J. Ryu and Y. M. Sung: Electrochem. Commun. **9** (2007) 1886–1891.
108) D. Q. Wei, Y. Zhou, D. C. Jia and Y. M. Wang: Surf. Coat. Technol. **201** (2007) 8715–8722.
109) T. Kokubo, F. Miyaji, H. M. Kim and T. Nakamura: J. Am. Ceram. Soc. **79** (1996) 1127–1129.
110) H. M. Kim, F. Miyaji, T. Kokubo and T. Nakamura: J. Mater. Sci. Mater. Med. **8** (1997) 341–347.
111) F. X. Qin, G. Q. Xie, X. M. Wang, T. Wada, M. Song, K. Furuya, M. Yoshimura, M. Tsukamoto and A. Inoue: Mater. Trans. **50** (2009) 1313–1317.
112) M. Yoshimura, S. E. Yoo, M. Hayashi and N. Ishizawa: Jpn. J. Appl. Phys. **28** (1989) L2007–L2009.
113) T. Onoki, X. M. Wang, S. L. Zhu, N. Sugiyama, Y. Hoshikawa, M. Akao, N. Matsushita, A. Nakahira, E. Yasuda, M. Yoshimura and A. Inoue: Mater. Sci. Eng. B **161** (2009) 27–30.
114) N. Sugiyama and M. Yoshimura: Mater. Sci. Eng. B **161** (2009) 31–35.
115) N. Sugiyama, H. Y. Xu, T. Onoki, Y. Hoshikawa, T. Watanabe, N. Matsushita, X. M. Wang, F. X. Qin, M. Fukuhara, M. Tsukamoto, N. Abe, Y. Komizo, A. Inoue and M. Yoshimura: Acta Biomater. **5** (2009) 1367–1373.
116) F. X. Qin, T. Wada, X. J. Yang, X. M. Wang, M. Yoshimura, K. Asami and A. Inoue: Mater. Trans. **51** (2010) 529–534.
117) M. Yoshimura, T. Onoki, M. Fukuhara, X. M. Wang, K. Nakata and T. Kuroda: Mater. Sci. Eng. B **148** (2008) 2–6.
118) J. J. Oak, G. W. Hwang, Y. H. Park, H. Kimura, S. Y. Yoon and A. Inoue: J. Biomed. Sci. Eng. **4** (2009) 384–391.
119) A. Nagai, K. Yamashita, S. Murayama, N. Matsushita, K. Okada, N. Abe, M. Tsukamoto, K. S. Son, X. M. Wang, G. Q. Xie and A. Inoue: Trans. JWRI **39** (2010) 306–307.
120) M. Tsukamoto, K. Asuka, H. Nakano, M. Hashida, M. Katto, N. Abe and M. Fujita: Vacuum **80** (2006) 1346–1350.
121) K. S. Son, E. S. Park, G. Q. Xie, X. M. Wang, M. Tsukamoto and A. Inoue: Proc. Visual-JW2010, ed. by Joining and Welding Research Institute, Osaka University, (2010) pp. 336–337.
122) H. F. Li, Y. B. Wang, Y. F. Zheng and J. P. Lin: J. Biomed. Mater. Res. B **100** (2012) 1721–1728.
123) W. Wang, R. Kokubun, K. Takakuda, S. L. Zhu and G. Q. Xie: H23 Year Book of Research Result Report, Research and Development Project on Advanced Materials Development and Integration of Novel Structured Metallic and Inorganic Materials, the Ministry of Education, Sports, Culture, Science and Technology, Japan, (2012) pp. 105–106.